Evaluation of decay times in coupled spaces: An efficient search algorithm within the Bayesian framework[a)]

Ning Xiang[b)] and Tomislav Jasa
School of Architecture and Department of Electrical, Computer, and Systems Engineering, Rensselaer Polytechnic Institute, Troy, New York 12180

(Received 9 June 2006; revised 16 September 2006; accepted 20 September 2006)

This paper discusses an efficient method for evaluating multiple decay times within the Bayesian framework. Previous works [N. Xiang and P. M. Goggans, J. Acoust. Soc. Am. **110**, 1415–1424 (2001); **113**, 2685–2697 (2003); N. Xiang, P. M. Goggans, T. Jasa, and M. Kleiner, **117**, 3707–3715 (2005)] have applied the Bayesian inference to cope with demanding tasks in estimating multiple decay times from Schroeder decay functions measured or calculated in acoustically coupled spaces. Since then a number of recent works call for efficient estimation methods within the Bayesian framework. An efficient analysis is of practical significance for better understanding and modeling the sound energy decay process in acoustically coupled spaces or even in single spaces for reverberation time estimation. This paper will first formulate the Bayesian posterior probability distribution function (PPDF) in a matrix form to reduce the dimensionality as applied to the decay time evaluation. Based on existence of only global extremes of PPDFs as observed from extensive experimental data, this paper describes a dedicated search algorithm for an efficient estimation of decay times. © *2006 Acoustical Society of America.* [DOI: 10.1121/1.2363932]

PACS number(s): 43.55.Br, 43.55.Mc [EJS] Pages: 3744–3749

I. INTRODUCTION

Recent research in acoustically coupled spaces[1–5] requires a set of practical tools to evaluate the sound energy decay from experimentally measured data or from computer-based simulations. One of the demanding tasks for better understanding and design of acoustics in coupled spaces lies in sound energy decay analysis. Applications of Bayesian probability theory in decay time evaluation in acoustically coupled spaces[6–8] have demonstrated a useful framework for analyzing Schroeder decay functions[9] from room impulse response measurements. The Bayesian framework proves to be able to estimate not only the decay parameters from Schroeder decay model,[6] but also to determine the decay order,[7] to quantify uncertainties of decay time estimates and the interrelationship between multiple decay times.[8]

Bayesian probability theory provides useful tools to formulate posterior probability density function (PPDF) of decay parameters. One approach to estimation of respective decay parameters is to localize global extremes of the PPDF over the parameter space, leading to an effective estimation of relevant decay parameters,[6] so-called maximum *a posterior* (MAP) estimation. Recent research in the acoustically coupled spaces demands an efficient way in performing Bayesian decay analysis. The subject of this paper is to show how one can accomplish the multiple decay time estimation with a low computation burden based on the MAP estimation. This effort is to speed up evaluations of relevant decay parameters from Schroeder decay functions using Bayesian probability theory. A practical significance of efficient methods is that architectural acousticians need to evaluate the multiple decay times over a number of octave/one-third octave bands, normally 5–20 evaluations to cover the frequency range of interest. For systematic investigations, a large number of room impulse responses need to be analyzed.

This paper is organized as follows, Sec. II briefly describes Bayesian formulation of posterior distributions over the decay time space. In Sec. II, one difference from previous work (Ref. 6), is the introduction of the Bayesian formalism in a matrix form, partially based on previous works.[10,11] This formulation along with that documented in Ref. 6 may piece together a coherent understanding of the model-based Bayesian inference, and help architectural acousticians to apply the Bayesian inference to the practical problems. On the application level the matrix formulation will particularly help those readers who want to implement the method using MATLAB. Section III discusses the proposed search method, its implementation and computation load evaluation. Finally, Sec. IV concludes the paper.

II. BAYESIAN FORMULATION

A. Schroeder decay models

This section begins with Schroeder decay function data $\mathbf{D}=[d_1,d_2,\ldots,d_K]^{Tr}$, a column vector of K elements, $()^{\mathrm{Tr}}$ stands for matrix transpose. A parametric model has been established based on the nature of Schroeder's integration[6,12]

$$\mathbf{D}=\mathbf{GA}+\mathbf{e}, \tag{1}$$

which approximates the data $\mathbf{D}$ with an error vector $\mathbf{e}$. $\mathbf{A}$ is a column vector of m coefficients, termed *linear parameter*

[a)]Aspects of this work have been presented at the 151st ASA Meeting, JASA **119** (2006), pp. 3208 (A).

[b)]Author to whom correspondence should be addressed; electronic mail: xiangn@rpi.edu

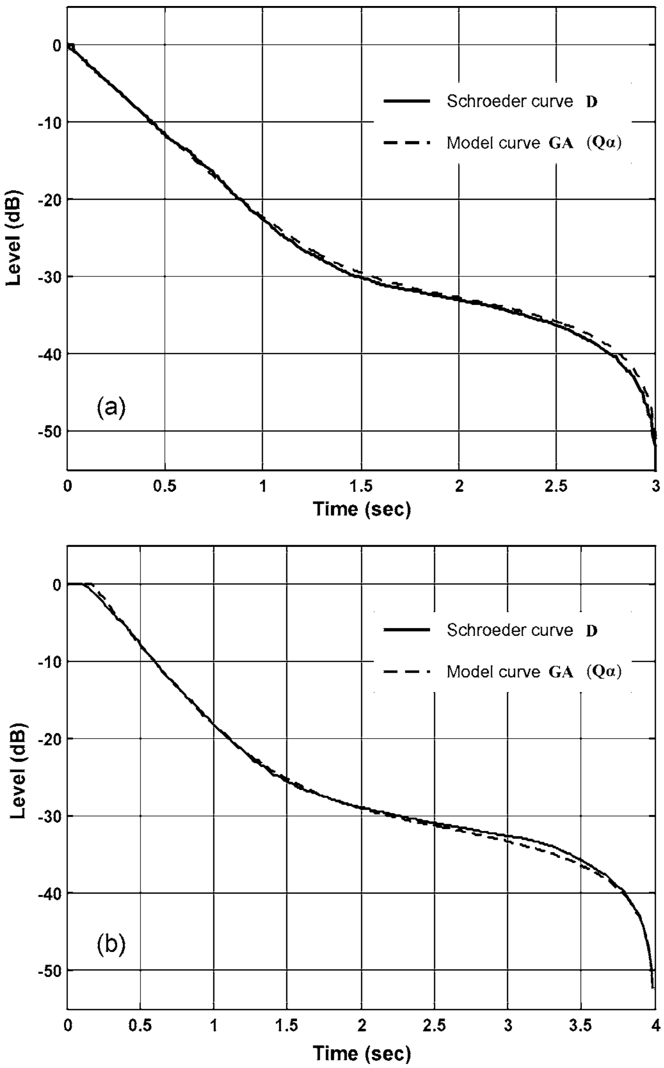

FIG. 1. Comparison between Schroeder decay function (**D**) measured in real halls and their model function (**GA**, or equivalently $\mathbf{Q}\boldsymbol{\alpha}$). (a) Room impulse response measured in Troy Savings Bank Music Hall, filtered at 500 Hz octave band. (b) Room impulse response measured in San. Patrick Church, filtered at 4 kHz ocatve band.

vector. **G** is a matrix of $K \times m$; jth column of **G** is given by

$$G_{kj}(T_j, t_k) = \begin{cases} t_K - t_k & \text{for } j = 0 \\ \exp(-13.8 \cdot t_k / T_j) & \text{for } 1, 2, \ldots, m-1, \end{cases} \tag{2}$$

where T_j is jth decay time to be determined for $0 \le j \le m-1$, $T_0 = \infty$. $0 \le k \le K-1$; t_K represents the upper limit of Schroeder's integration. Recent works[8,12] have experimentally proven the validity of this model, especially when t_K is large enough. Figure 1 illustrates two examples of the Schroeder decay function **D** calculated from real hall measurements and its model function **GA** with properly estimated model parameters.

The decay model in Eq. (1) is in the form of generalized linear models.[10,11] This special form has gained general interest since one can analytically formulate the PPDF within the Bayesian framework in a tractable form. To proceed, an eigen decomposition of $m \times m$ square matrix $\mathbf{G}^{\mathbf{Tr}}\mathbf{G}$ comes into use:

$$\mathbf{G}^{\mathbf{Tr}}\mathbf{G} = \mathbf{E}\boldsymbol{\Lambda}\mathbf{E}^{\mathbf{Tr}}, \tag{3}$$

where $()^{\mathrm{Tr}}$ represents matrix transpose, **E** is a square matrix containing m eigenvectors, while $\boldsymbol{\Lambda}$ is a diagonal matrix containing m eigenvalues of the eigenvectors. The eigen decomposition facilitates converting **G** into an orthonormalized one **Q** or vice versa (see Appendix A):

$$\mathbf{Q} = \mathbf{G}\mathbf{E}\boldsymbol{\Delta}^{-1}; \quad \mathbf{G} = \mathbf{Q}\boldsymbol{\Delta}\mathbf{E} \tag{4}$$

with

$$\boldsymbol{\Delta}^{\mathbf{Tr}}\boldsymbol{\Delta} = \boldsymbol{\Lambda}. \tag{5}$$

In similar fashion, the linear parameter vector **A** can be converted into the orthonormalized one $\boldsymbol{\alpha}$, or vice versa:

$$\boldsymbol{\alpha} = \boldsymbol{\Delta}\mathbf{E}\mathbf{A}; \quad \mathbf{A} = \mathbf{E}\boldsymbol{\Delta}^{-1}\boldsymbol{\alpha}, \tag{6}$$

such that the error function **e** can be equivalently expressed in terms of Schroeder decay function **D** and the orthonormalized model $\mathbf{Q}\boldsymbol{\alpha}$:

$$\mathbf{e} = \mathbf{D} - \mathbf{Q}\boldsymbol{\alpha}. \tag{7}$$

B. Bayesian decay parameter estimation

Bayesian theory formulates the PPDF through the prior probability density and likelihood function via Bayes' theorem:

$$p(\mathbf{A}, \mathbf{T} | \mathbf{D}, I) = \frac{p(\mathbf{A}, \mathbf{T} | I) p(\mathbf{D} | \mathbf{A}, \mathbf{T}, I)}{p(\mathbf{D} | I)}, \tag{8}$$

where $p(\mathbf{D}|I)$ acts in the context of decay time estimation as a normalization constant. **T** is a vector matrix of m coefficients, termed *nonlinear parameter vector*. $p(\mathbf{A}, \mathbf{T}|I)$ is the prior distribution function of **A** and **T**. Bayes' theorem in Eq. (8), therefore, represents how our prior knowledge $p(\mathbf{A}, \mathbf{T}|I)$ is modified in presence of data through the likelihood function $p(\mathbf{D}|\mathbf{A}, \mathbf{T}, I)$. Background information I includes that the Schroeder decay model in Eq. (2) through Eq. (1) describes the data **D** reasonably well so that all errors in **e** are bounded by a finite value. Given finite errors and a reasonable model as the only available information, application of the principle of the maximum entropy[6] assigns a Gaussian distribution to the likelihood function $p(\mathbf{D}|\mathbf{A}, \mathbf{T}, I)$ and an independence to errors e_i from each other, so that

$$p(\mathbf{D} | \mathbf{A}, \mathbf{T}, \sigma, I) = (\sqrt{2\pi}\sigma)^{-K} \exp\left(\frac{\mathbf{e}^{\mathbf{Tr}}\mathbf{e}}{2\sigma^2}\right), \tag{9}$$

with a finite, but unspecified error variance σ^2. The likelihood function $p(\mathbf{D}|\mathbf{A}, \mathbf{T}, \sigma, I)$ implies that the error variance σ^2 at this stage is still unknown.

A substitute of Eq. (7) into Eq. (9) yields the posterior probability density function $p(\boldsymbol{\alpha}, \mathbf{T}|\mathbf{D}, \sigma, I)$ in terms of the likelihood $p(\mathbf{D}|\boldsymbol{\alpha}, \mathbf{T}, \sigma, I)$ and prior probability function $p(\boldsymbol{\alpha}, \mathbf{T}|I)$:

$$p(\boldsymbol{\alpha}, \mathbf{T} | \mathbf{D}, \sigma, I) \propto p(\boldsymbol{\alpha}, \mathbf{T} | I)(\sqrt{2\pi}\sigma)^{-K} \times \exp\left[-\frac{(\mathbf{D} - \mathbf{Q}\boldsymbol{\alpha})^{\mathbf{Tr}}(\mathbf{D} - \mathbf{Q}\boldsymbol{\alpha})}{2\sigma^2}\right], \tag{10}$$

where $p(\boldsymbol{\alpha}, \mathbf{T}|\mathbf{D}, \sigma, I)$ and $p(\boldsymbol{\alpha}, \mathbf{T}|I)$ reflect the fact that the

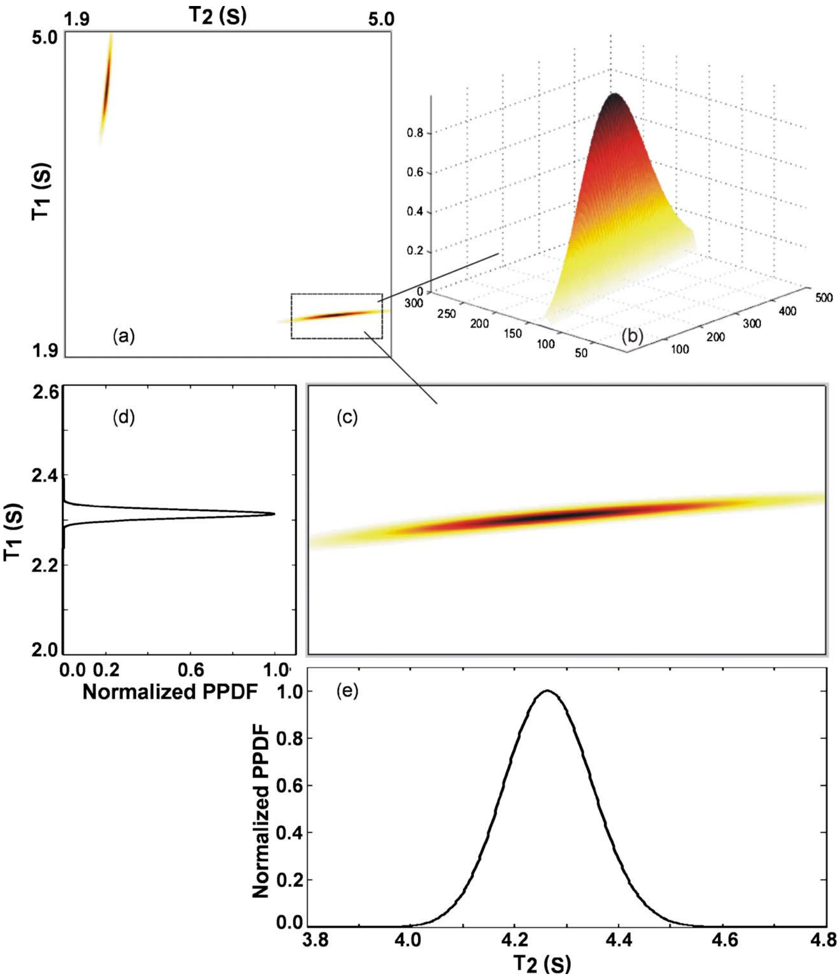

FIG. 2. (Color online) Posterior probability density function (PPDF) over decay time space $\{T_1, T_2\}$ evaluated for the room impulse response measured in San. Patrick Church as shown in Fig. 1(b). The PPDF in 2D presentation between 1.9 and 5.0 s. (b) One of the PPDF mode in three-dimensional (3D) presentation over $\{2.0s, 2.6s\}$ and $\{3.8s, 4.8s\}$ with a grid of 300×500. (c) One of the PPDF mode in 2D presentation over $\{2.0s, 2.6s\}$ and $\{3.8s, 4.8s\}$. (d), (e) Projections onto two decay time axes from slices across the peak of the mode.

equivalent orthonormalized model $\mathbf{Q}\boldsymbol{\alpha}$ has substituted the Schroeder decay model $\mathbf{GA}$ through Eqs. (4), (6), and (7), so the linear vector $\mathbf{A}$ has been substituted by $\boldsymbol{\alpha}$.

The marginalization over $\boldsymbol{\alpha}$ with a uniform prior, and over σ by assigning Jeffreys' prior along with the orthonormalization stated in Sec. II A lead to an analytically tractable PPDF in the form of the student-T distribution (see Appendix B):

$$p(\mathbf{T}|\mathbf{D},I) \propto [\mathbf{D}^{\mathrm{Tr}}\mathbf{D} - \mathbf{q}^{\mathrm{Tr}}\mathbf{q}]^{(m-K)/2}, \tag{11}$$

with

$$\mathbf{q} = \mathbf{Q}^{\mathrm{Tr}}\mathbf{D} \tag{12}$$

Similar to the formulation in Ref. 7, the marginalization removes $\boldsymbol{\alpha}$ and σ from the current problem, and results in the student-T PPDF over only the decay time space. The decay time estimation can, therefore, be carried out in a dramatically reduced dimensionality. Once the decay times are estimated, an expected linear parameter vector $\langle \mathbf{A} \rangle$ can be determined through Eq. (6) and $\langle \boldsymbol{\alpha} \rangle = \hat{\mathbf{q}}$ with $\hat{\mathbf{q}}$ being a MAP estimate of $\mathbf{q}$ in Eq. (12).

C. Numerical examples

Figure 1(a) shows the Schroeder decay function $\mathbf{D}$ of 3000 elements within 500 Hz (oct) measured in the Troy Savings Bank Music Hall, Troy, NY, and the decay model $\mathbf{GA}$

$$\mathbf{GA} = \begin{pmatrix} t_K - t_0 & e^{-13.8 \cdot t_0/T} \\ t_K - t_1 & e^{-13.8 \cdot t_1/T} \\ \vdots & \vdots \\ t_K - t_{K-1} & e^{-13.8 \cdot t_{K-1}/T} \end{pmatrix} \begin{pmatrix} 4.339E-7 \\ 1.002 \end{pmatrix} \tag{13}$$

with K=3000, reverberation time T=2.60 s. Figure 1(b) shows the Schroeder decay function $\mathbf{D}$ of 4000 elements measured in San. Patrick Church, Watervliet, NY, and the decay model $\mathbf{GA}$

$$\mathbf{GA} = \begin{pmatrix} t_K - t_0 & e^{-13.8 \cdot t_0/T_1} & e^{-13.8 \cdot t_0/T_2} \\ t_K - t_1 & e^{-13.8 \cdot t_1/T_1} & e^{-13.8 \cdot t_1/T_2} \\ \vdots & \vdots & \vdots \\ t_K - t_{K-1} & e^{-13.8 \cdot t_{K-1}/T_1} & e^{-13.8 \cdot t_{K-1}/T_2} \end{pmatrix} \times \begin{pmatrix} 2.168E-7 \\ 2.596 \\ 0.205 \end{pmatrix}, \tag{14}$$

with K=4000, decay times T_1=2.29 s, T_2=4.21 s.

Figure 2 illustrates normalized PPDFs over decay time space $\{T_1, T_2\}$ given the model in Eq. (14) and the measured Schroeder decay function $\mathbf{D}$ as shown in Fig. 1(b). The PPDF over a two-dimensional (2D) decay time space between 1.9 and 5 s includes two distinct, well-separated distribution modes of equal height. Figures 2(d) and 2(e) illustrate the projections onto two decay time axes from slices

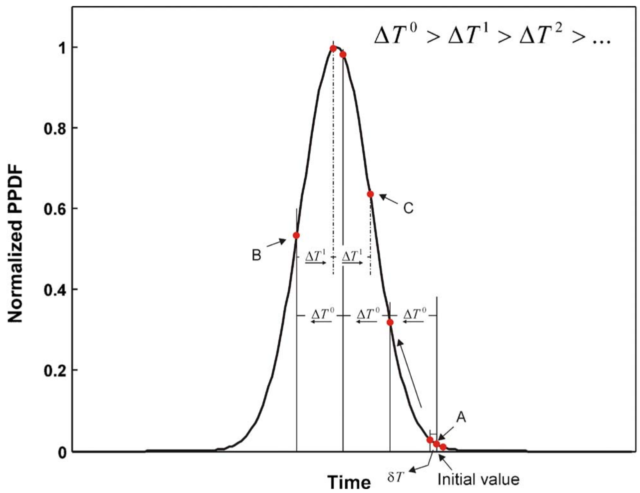

FIG. 3. (Color online) Search method within one-dimensional parameter space. Point "A" represents the starting sample determined by a random set of decay times (initial value). Two more samples with the smallest step size δT determine the up-hill moving direction along which a large step size ΔT^0 is kept until point "B". Then a reduced step size ΔT^1 and an opposite moving direction are kept until point "C". From point C the moving direction will be reversed with an even smaller step size ΔT^2, and so on.

across the peak of the mode. Extensive evaluations of a large number of measured results confirm that the student-T distribution in Eq. (11) over n-dimensional decay time space demonstrates $n!$ distinctly separated distribution modes of equal height.[6,7] For this reason, only one mode serves the estimation purpose. Besides these modes, no local extremes so far have been found. This fact gives a rise to a simplified search algorithm elaborated in the following: localization of the peak position of one of these modes will serve estimation of decay times.[13]

III. A FAST SEARCH ALGORITHM

The PPDF associated with any particular set of values for the decay parameters is a measure of how much one believes that they really lie in the neighborhood of that range. Therefore, localization of one of the PPDF global extremes in the parameter space will lead to an effective estimation of relevant decay parameters,[6] the MAP estimation. Previous works have applied Gibbs sampling technique[6,14] within the Bayesian framework. Gibbs sampler breaks the problem of drawing samples from a multivariante density down to densities of smaller dimensionality in a rotational pattern. Gibbs sampler may still require a large number of random samples within each single rotation process. In Bayesian decay analysis, however, one can exploit the fact that the student-T distribution within the subspace of a single mode will not exhibit local extremes, which means that there is only one "hill" along one decay-time axis within the subspace around the single mode.

A. Search algorithm

Inspired by the rotational pattern of the Gibbs sampler, one begins a search along one decay-time axis while fixing the others. At the initial point, randomly chosen value of T_i with its PPDF sample indicated by point "A" in Fig. 3, a proper moving direction can be estimated by comparing PPDF values in Eq. (11) at two other adjacent T_i's on each side with a tiny step size, *the smallest step size* δT (defined according to required precision prior to the search). After determination of the moving "up-hill" direction, a relative large step size (termed *initial step size* ΔT^0 within each iteration in this paper) is recommended to search the one dimensional space coarsely. The same step size is kept until the PPDF value becomes smaller than the previous one as indicated by point "B" in Fig. 3. This causes reversing of the moving direction and decreasing of the step size $\Delta T^1 < \Delta T^0$; with this moving direction and step size the search goes until the point "C" in Fig. 3. Conceivably both the moving-direction reversion and the step-size reduction could happen many times until the step size becomes the smallest one (δT) as initially defined. With this smallest step size one more search along the corresponding moving direction keeps going up hill until the PPDF value turns "down hill," and the search within this dimension can be stopped. By fixing the value of the last T_i^1, the search goes on to the next one-dimensional space of T_{i+1}, if any, until all the dimensions are searched; this finishes up one iteration (rotation) with $T_1^1, T_2^1, \ldots$.All T_i^1s and their corresponding PPDF values are kept in the memory of the search algorithm.[15–20]

The next iteration begins with $T_1^1, T_2^1, \ldots$ as initial values. A breaking mechanism to stop overall search can be determined by the fact that the (large) step size is reduced to the smallest step size $\Delta T^n = \delta T$ and differences between the current PPDF value and the previous one fall below a threshold Δp as defined according to the required precision. The decay time values associated with the maximum value of the PPDF determined by Eq. (11) among the search iterations will be kept as the MAP estimates.

B. Implementation and discussion

Previous work[8] shows very different, varied shapes of PPDF modes from data to data. In double-slope cases, in particular, often the PPDF mode along one dimension can be so different from the one along the other dimension over the decay time space, so that there will not be general rules of how the initial step size, the step size reduction can be selected. Experimental results as shown in this paper use the following values

- The smallest step size: $\delta T = 1.0 \times 10^{-4}$ s
- The initial (large) step size: $\Delta T^0 = X \cdot \delta T$ with an initial step size factor $X = 81$
- The step size factor X reduces for ΔX when reserving the search direction: At the first direction reversion $\Delta X = 10$, the step size factor becomes $X - \Delta X$, ΔX reduces 2 at every direction reversion until $\Delta X = 1$ or $X = 1$
- The threshold of the PPDF difference: $20 lg(\Delta p) = 2.0 \times 10^{-3}$

This work calculates the Schroeder decay functions from room impulse responses at an integration interval of 1 ms, which results in Schroeder decay functions of several hundreds till several thousand points [with K in Eq. (11) being on order of 10^3]. For this reason the calculation of the PPDF

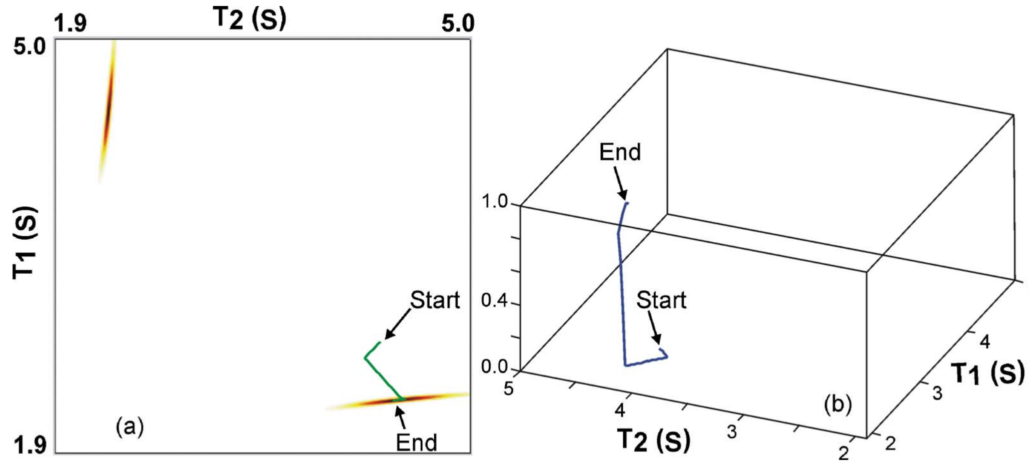

FIG. 4. (Color online) Search trace over decay time space $\{T_1, T_2\}$ evaluated for the experimental data measured in San. Patrick Church as shown in Fig. 2. The MAP values $T_1=2.29$ s, $T_2=4.21$ s as from iteration 28. (a) Search trace overlapped with the 2D PPDF over the decay time space $\{T_1, T_2\}$ between 1.9 and 5.0 s. (b) Search trace in a 3D presentation.

using Eq. (11) is conveniently pursued on a logarithmic basis $20lg[p(\mathbf{T}|\mathbf{D},\mathbf{I})]$, where quantity $\mathbf{D}^{\mathbf{Tr}}\mathbf{D}$ needs to be calculated only once throughout the overall search. Figure 4 illustrates the search iterations for a double-slope case of the experimental data shown in Fig. 2. Figure 4(a) shows its search trace overlayed on top of the 2D presentation of the PPDF over the decay time space of $\{1.9s, 5.0s\}$, while Fig. 4(b) illustrates how the search iteratively climbs one of the PPDF modes upwards.

The dynamic step-size reduction has been proven to be a reasonable way to reduce the computational load while achieving high search resolution. As demonstrated by this numerical example, 28 iterations for the double-slope case converge the search; each iteration requires only a few of search steps, while the search with a fixed step size as small as δT will require hundreds, even thousands of the small steps, especially when the random sampling begins in ranges where the PPDF is of low values. The single-slope cases using the dynamic step-size reduction often require significantly less search effort, since only a few of the step-size reductions associated with search direction reversions within one single iteration are needed. Using traditional Gibbs sampling,[6,10] however, a relatively large number of samples have to be evaluated within each iteration, in order of thousand samples, since the PPDF shape within each iteration is in general not known.

The search algorithm with the dynamic step-size reduction as implemented in this work runs efficiently, usually takes a few seconds for double-slope cases on a currently available personal computer when the Schroeder decay data are in order of thousands points, while for single-slope cases it usually takes less than 1 s or less. The search process also has a "burn-in" phase like other classical Markov Chain Monte Carlo methods.[10] The burn-in process can be significantly shortened by a simple estimate of T_1^0 using a small portion of the Schroeder decay function, say between -5 and -10 dB, particularly for the single-slope case. In this work an initial value of $T_2^0=1.5\times T_1^0$ is always set for the double-slope case. The search algorithm itself is then not a random process at all. When starting at the same initial point in the decay time space, the search algorithm will converge at the same ending point given the step sizes, the reduction size and the breaking threshold as mentioned above.

Note that there might be even more efficient algorithms for this specific application, if substantial optimization would be undertaken. In addition, only in this specific application, the search algorithm can be effected. If the PPDF over the parameter space of other applications shows not only the global extreme, but is accompanied by possible local extremes, one should resort to the traditional Gibbs sampling method or other Markov Chain Monte Carlo methods.

IV. CONCLUSIONS

This work exploits the Schroeder decay function model which is in the form of the generalized linear models. This specific model form makes it possible to reduce the dimensionality of the posterior probability distribution functions (PPDFs) within the Bayesian framework by probabilistic marginalization to a compact form termed student-T distribution. This paper derives the student-T distribution in a matrix form. At the end, the student-T distribution is a function of only decay times and there are only global extremes over the decay time space, so as to implement a dramatically simplified search algorithm. Inspired by rotational patterns of Gibbs sampling, a dynamic reduction of search step sizes with similar rotational iterations results in an efficient search algorithm for the Bayesian decay time estimation. When the PPDF contains not only global extremes, but is accompanied by possible local extremes, more general approaches such as Markov Chain Monte Carlo methods should be applied.

ACKNOWLEDGMENTS

The authors would like to thank Dr. Paul Goggans and Dr. Kevin Knuth for their valuable discussion and advice. The authors would also like to express their gratitude to Dr. Chris Jaffe, Dr. Mendel Kleiner, and Dr. Rendell R. Torres, who supported this work with enthusiasm, to Donghua Li and Zühre Sü, who participated in extensive room-acoustic data collection in the scope of their M.S. Degree theses.

APPENDIX A

$\mathbf{E}$ of Eq. (3) has following properties:

$$\mathbf{E}^{\mathbf{Tr}} = \mathbf{E}; \quad \mathbf{E}^{\mathbf{Tr}}\mathbf{E} = \delta, \tag{A1}$$

where δ is an identity matrix. Using Eqs. (3)–(5) one can derive that

$$\mathbf{Q}^{\mathbf{Tr}}\mathbf{Q} = \delta. \tag{A2}$$

APPENDIX B

From Eqs. (10), (12), and (A2)

$$\begin{aligned}(\mathbf{D} - \mathbf{Q}\boldsymbol{\alpha})^{\mathbf{Tr}}(\mathbf{D} - \mathbf{Q}\boldsymbol{\alpha}) &= \mathbf{D}^{\mathbf{Tr}}\mathbf{D} - \boldsymbol{\alpha}^{\mathbf{Tr}}\mathbf{Q}^{\mathbf{Tr}}\mathbf{D} - \mathbf{D}^{\mathbf{Tr}}\mathbf{Q}\boldsymbol{\alpha} + \boldsymbol{\alpha}^{\mathbf{Tr}}\mathbf{Q}^{\mathbf{Tr}}\mathbf{Q}\boldsymbol{\alpha} \\ &= (\mathbf{D}^{\mathbf{Tr}}\mathbf{D} - \mathbf{q}^{\mathbf{Tr}}\mathbf{q}) + (\boldsymbol{\alpha} - \mathbf{q})^{\mathbf{Tr}}(\boldsymbol{\alpha} - \mathbf{q})\end{aligned} \tag{B1}$$

$$p(\boldsymbol{\alpha},\mathbf{T}|\mathbf{D},\sigma,I) \propto (\sqrt{2\pi}\sigma)^{-K}\exp\left[\frac{-(\mathbf{D}^{\mathbf{Tr}}\mathbf{D} - \mathbf{q}^{\mathbf{Tr}}\mathbf{q})}{2\sigma^2}\right] \times\exp\left[-\frac{(\boldsymbol{\alpha} - \mathbf{q})^{\mathbf{Tr}}(\boldsymbol{\alpha} - \mathbf{q})}{2\sigma^2}\right]. \tag{B2}$$

The marginalization over the nuisance parameters $\boldsymbol{\alpha}$ by assigning a uniform prior $p(\boldsymbol{\alpha}|\mathbf{I})=\text{const}$, $p(\mathbf{T}|\boldsymbol{\alpha},\mathbf{I})=\text{const}$:

$$p(\mathbf{T}|\mathbf{D},\sigma,\mathbf{I}) \propto \int_{-\infty}^{\infty} p(\boldsymbol{\alpha},\mathbf{T}|\mathbf{D},\sigma,\mathbf{I})d\boldsymbol{\alpha}. \tag{B3}$$

$$p(\mathbf{T}|\mathbf{D},\sigma,I) \propto (\sqrt{2\pi}\sigma)^{-K+m} \times\int_{-\infty}^{\infty} \exp\left[\frac{-(\mathbf{D}^{\mathbf{Tr}}\mathbf{D} - \mathbf{q}^{\mathbf{Tr}}\mathbf{q})}{2\sigma^2}\right]d\boldsymbol{\alpha}, \tag{B4}$$

according to Eq. (A5) in Ref. 6:

$$\int_{-\infty}^{\infty} \exp\left[\frac{-(\boldsymbol{\alpha} - \mathbf{q})^{\mathbf{Tr}}(\boldsymbol{\alpha} - \mathbf{q})}{2\sigma^2}\right]d\boldsymbol{\alpha} = (\sqrt{2\pi}\sigma)^{m} \tag{B5}$$

and an integration of Eq. (B4) over σ by assigning Jeffrey's prior $1/\sigma^6$ yields Eq. (11).

[1] J. S. Anderson, M. Bratos-Anderson, and P. Doany, "The acoustics of a large space with a repetitive pattern of coupled rooms," J. Sound Vib. **208**, 313–329 (1997).

[2] J. E. Summers, R. R. Torres, and Y. Shimizu, "Statitical-acoustics models of energy decay in systems of coupled rooms and their relation to geometrical acoustics," J. Acoust. Soc. Am. **116**, 958–969 (2004).

[3] J. E. Summers, R. R. Torres, Y. Shimizu, and Bengt-Inge L. Dalenbäck, "Adapting a randomized beam-axis-tracing algorithm to modeling of coupled rooms via late-part ray tracing," J. Acoust. Soc. Am. **118**, 1491–1502 (2005).

[4] D. T. Bradley and L. M. Wang, "The effects of simple coupled volume geometry on the objective and subjective results from nonexponential decay," J. Acoust. Soc. Am. **118**, 1480–1490 (2005).

[5] V. Valeau, J. Picaut, and M. Hodgson, "On the use of a diffusion equation for room-acoustic predictions," J. Acoust. Soc. Am. **119**, 1504–1513 (2006).

[6] N. Xiang and P. M. Goggans, "Evaluation of decay times in coupled spaces: Bayesian parameter estimation," J. Acoust. Soc. Am. **110**, 1415–1424 (2001).

[7] N. Xiang and P. M. Goggans, "Evaluation of decay times in coupled spaces: Bayesian decay model selection," J. Acoust. Soc. Am. **113**, 2685–2697 (2003).

[8] N. Xiang, P. M. Goggans, T. Jasa, and M. Kleiner, "Evaluation of decay times in coupled spaces: Reliability analysis of Bayesian decay time estimation," J. Acoust. Soc. Am., **117**, 3705–3715 (2005).

[9] M. R. Schroeder, "New method of measuring reverberation time," J. Acoust. Soc. Am. **37**, 409–412 (1965).

[10] J. J. K. O'Ruanaidh and W. J. Fitzgerald, *Numerical Bayesian Methods Applied to Signal Processing* (Springer, New York, 1996).

[11] G. L. Bretthorst, "Bayesian analysis. I. Parameter estimation using quadrature NMR models," J. Magn. Reson. (1969-1992) **88**, 533–551 (1990).

[12] N. Xiang, "Evaluation of reverberation times using a non-linear regression approach," J. Acoust. Soc. Am. **98**, 2112–2121 (1995).

[13] S. Dosso, "Quantifying uncertainty in geoacoustic inversion. I. A fast Gibbs sampler approach," J. Acoust. Soc. Am. **111**, 129–142 (2002).

[14] Z. H. Michalopoulou and M. Picarelli, "Gibbs sampling for time-delay and amplitude estimation in underwater acoustics," J. Acoust. Soc. Am. **117**, 799–808 (2005).

[15] E. T. Jaynes, *Probability Theory: The Logic of Science* (Cambridge University Press, Cambridge, 2003).

[16] F. Jacobsen, "A note on acoustic decay measurements," J. Sound Vib. **115**, 165–170 (1987).

[17] M. Vorländer and H. Bietz, "Comparison of methods for measuring reverberation time," Acustica **80**, 205-215 (1994).

[18] A. Lundeby, T. E. Vigran, H. Bietz, and M. Vorländer, Uncertainties of measurements in room acoustics," Acustica **81**, 344–355 (1995).

[19] D. S. Sivia, *Data Analysis: A Bayesian Tutorial* (Clarendon Press, Oxford, 1996).

[20] H. Jeffreys, *Theory of Probability*, 3rd ed. (Oxford University Press, London, 1961).